Eur. Phys. J. D **46**, 409–414 (2008)
DOI: 10.1140/epjd/e2007-00310-7

THE EUROPEAN PHYSICAL JOURNAL D

Coincidence studies of electron impact ionization of atomic inner shells

J. Martinez[1,a], C.T. Whelan[1], and H.R.J. Walters[2]

[1] Physics Department, Old Dominion University, Norfolk, Virginia, 23529-0116, USA
[2] Department of Applied Mathematics and Theoretical Physics, The Queen's University, Belfast, BT7 1NN, UK

Received 25 July 2007 / Received in final form 20 September 2007
Published online 14 November 2007 –

Abstract. We consider $(e, 2e)$ processes on the $2s$ and $2p$ shells of argon and magnesium. We present triple differential cross sections in coplanar asymmetric geometry calculated in the Plane Wave Born, 1st Born and Distorted Wave Born approximations. We show that the currently available relative experiments can not easily distinguish between these approximations. We make proposals for relative experiments where the difference between these approaches can be more readily observed.

PACS. 34.80.Dp Atomic excitation and ionization by electron impact – 34.80.Pa Coherence and correlation in electron scattering – 34.50.Fa Electronic excitation and ionization of atoms

Because of the smallness of the inner-shell cross sections it is only in recent years that experimental techniques have become sufficiently refined to make viable inner shell $(e, 2e)$ measurements. In this paper we are concerned with the ionization from the $2s$ and $2p$ shells of Ar and Mg.

The first $(e, 2e)$ measurement on Ar$(2p)$ [1] were made by Lahmam-Bennani et al. [2] at an impact energy of 8 keV with further results being reported by [3–5], and at significantly lower impact energies by [6]. Very recently new experimental data has become available for Ar$(2s)$, Mg$(2s)$ and Mg$(2p)$, at impact energies of the order of 1 keV [7].

The physics one sees in a coincidence experiment is predicated on the choice of geometry. The experiments, to-date, have been performed in coplanar asymmetric geometry, (Fig. 1). This choice of geometry has been a favorite for experimental studies since being introduced by Ehrhardt and his collaborators in one of the very first $(e, 2e)$ experiments. This choice of kinematics is ideal for the application of perturbation theory to atomic outer shells (for a review see [8]). A further feature of the reported inner shell experiments is that they are all relative. Putting $(e, 2e)$ data, taken in the gas phase, on an absolute scale is an enormously difficult task, see e.g. [9,10], consequently it is of value to search out kinematics where the difference between the theoretical approaches is clearly visible in the shape of the cross sections. This is one of the primary purposes of this paper.

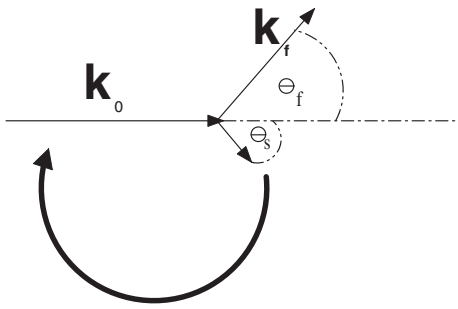

Fig. 1. Coplanar asymmetric geometry. An electron, momentum, $\mathbf{k}_0$ is incident on an atom and two electrons are detected with their angles and energies resolved left and right of the beam direction, the faster of the two with momentum $\mathbf{k}_f$ is detected at an angle of magnitude θ_f measured in an anticlockwise direction with respect to the beam direction; the slower electron with an angle, θ_s measured in a clockwise direction with respect to the beam has momentum $\mathbf{k}_s$.

1 Theory

The Distorted Wave Born Approximation, DWBA, [11–13] offers a straightforward and flexible approach to the calculation of $(e, 2e)$ processes. It has proved particularly useful in identifying targets and kinematics where multiple scattering effects are important [6,13,14]. In this paper we will study the inner shell ionization of argon and magnesium using the full flexibility of the approximation to explore the ionization mechanisms.

[a] e-mail: jmart044@odu.edu

In atomic units ($\hbar = m_e = e = 1$) the triple differential cross section, TDCS, in the DWBA approximation for closed shell atoms is of the form [12,13,15],

$$\frac{d^3\sigma^{DWBA}}{d\Omega_f d\Omega_s dE} = (2\pi)^4 \frac{k_f k_s}{k_0} \sum_m |f_{nlm}|^2 + |g_{nlm}|^2 - \Re e(f^*_{nlm} g_{nlm}). \quad (1)$$

The direct and exchange amplitudes are respectively

$$f_{nlm} = \langle \chi_a^-(\mathbf{k}_f, \mathbf{r}_f)\chi_b^-(\mathbf{k}_s, \mathbf{r}_s) \times |\frac{1}{\|\mathbf{r}_f - \mathbf{r}_s\|}|\chi_0^+(\mathbf{k}_f, \mathbf{r}_f)\psi_{nlm}(\mathbf{r}_s)\rangle \quad (2)$$

$$g_{nlm} = \langle \chi_a^-(\mathbf{k}_f, \mathbf{r}_s)\chi_b^-(\mathbf{k}_s, \mathbf{r}_f) \times |\frac{1}{\|\mathbf{r}_f - \mathbf{r}_s\|}|\chi_0^-(\mathbf{k}_f, \mathbf{r}_f)\psi_{nlm}(\mathbf{r}_s)\rangle \quad (3)$$

where we have used the notation of [15]. In the absence of any distorting potentials the distorted waves, χ, reduce to plane waves. In the extreme case when there is no distorting potentials acting on any of the electrons then we have the PWPWPW, or purely plane wave, case

$$f_{nlm}^{PWPWPW} = (2\pi)^{-\frac{9}{2}} \int d^3r_s d^3r_f e^{-i\mathbf{k}_f\cdot\mathbf{r}_f} e^{-i\mathbf{k}_s\cdot\mathbf{r}_s} \times \frac{1}{\|\mathbf{r}_f - \mathbf{r}_s\|} e^{i\mathbf{k}_0\cdot\mathbf{r}_f}\psi_{nlm}(\mathbf{r}_s). \quad (4)$$

Now if we apply the Bethe integral relation

$$\int d^3r_f \frac{e^{i\mathbf{q}\cdot\mathbf{r}_f}}{\|\mathbf{r}_f - \mathbf{r}_s\|} = \frac{4\pi}{q^2} e^{i\mathbf{q}\cdot\mathbf{r}_s} \quad (5)$$

equation (4) becomes:

$$f_{nlm}^{PWPWPW} = \frac{4\pi}{(2\pi)^{\frac{9}{2}} q^2} \int d^3r e^{i\mathbf{p}\cdot\mathbf{r}}\psi_{nlm}(\mathbf{r}) \quad (6)$$

where $\mathbf{q} = \mathbf{k}_0 - \mathbf{k}_f$ and $\mathbf{p} = \mathbf{q} - \mathbf{k}_s$. If we can neglect the exchange amplitude then we have

$$\frac{d^3\sigma^{PW}}{d\Omega_f d\Omega_s dE} = (2\pi)^4 \frac{k_f k_s}{k_0} \sum_m (|f_{nlm}^{PW}|^2) \quad (7)$$

$$= \frac{k_f k_s}{2\pi^3 (q)^4 k_0} \sum_m |\int d^3r_s e^{i\mathbf{p}\cdot\mathbf{r}_s}\psi_{nlm}(\mathbf{r}_s)|^2. \quad (8)$$

We immediately recognize the term $\int d^3r_s e^{i\mathbf{p}\cdot\mathbf{r}_s}\psi_{nlm}(\mathbf{r}_s)$ as the atomic wave function in momentum space $\hat{\psi}_{nlm}(\mathbf{p})$. Equation (8) defines the plane wave Born approximation, (PWBA). The TDCS in the PWBA is thus crucially dependent on the norm of the target wave function summed over the magnetic quantum numbers m, and the vector $\mathbf{p}$. As is well-known, [16,17], the momentum space wave function may be written $\hat{\psi}_{nlm}(\mathbf{p}) = F_{nl}(p)Y_{lm}(\hat{\mathbf{p}})$ where

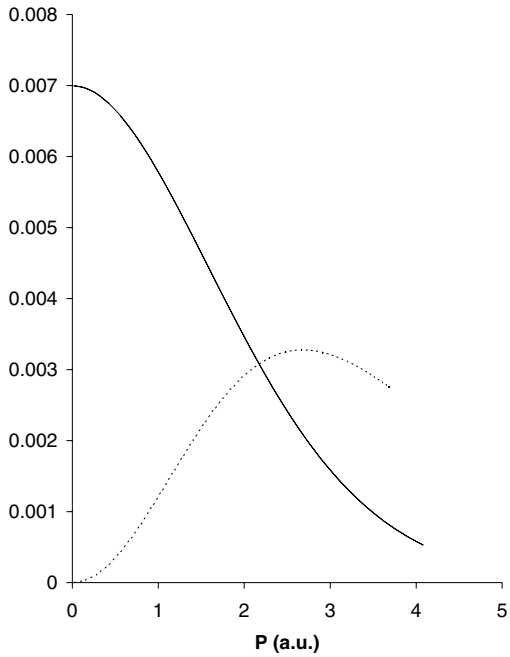

Fig. 2. The TDCS calculated in the PWPWPW approximation, (4) for coplanar asymmetric geometry plotted as a function of $p = \|k_0 - k_f - k_s\|$ where the fast electron having an energy of 500 eV. The solid curve is argon $2s$, with a slow electron energy of 56 eV and $\theta_f = 4°$. The dotted curve is argon $2p$, with a slow electron energy of 46 eV and $\theta_f = 8°$.

the angular dependence is entirely in the spherical harmonics, and F_{nl} is independent of m. Consequently (8) may be written:

$$\frac{d^3\sigma^{PW}}{d\Omega_f d\Omega_s dE} = (2\pi)^4 \frac{k_f k_s (|F_{nl}(p)|^2)}{k_0} \sum_m |Y_{lm}|^2. \quad (9)$$

Now

$$\sum_m |Y_{lm}|^2 = \frac{2l+1}{4\pi} \quad (10)$$

(an elementary proof of (10) is given in Appendix below). The TDCS depends only on the magnitude of $\mathbf{p}$ through $F_{nl}(p)$. The character of the target wave function is most clearly seen in the region of $\mathbf{p} = \mathbf{0}$.

This corresponds to

$$\mathbf{q} - \mathbf{k}_s = \mathbf{0} \Rightarrow \mathbf{k}_s = \mathbf{k}_0 - \mathbf{k}_f \quad (11)$$

i.e. zero recoil of the ion. We take (11) as the defining equation for the Bethe Ridge. In Figure 2 we present the TDCS as a function of $p = \|\mathbf{p}\|$ calculated in the PW-PWPW Approximation, (4), for Ar($2s$) and Ar($2p$). The cross section has a minimum at $p = 0$ for the $2p$ case but a maximum for $2s$ at the same point. This behavior is characteristic of the state of the target, i.e. for an electron in an s state the most probable momentum is zero, while this is the least probable momentum value for a p electron [16,18,19]. The $2p$ case exhibits a maximum for some value of $p = p_0$ and then declines uniformly. If the kinematics of our experiment are such that we can reach

values of $p > p_0$ and p_{max} is the maximum value of p that can be obtained then we will find a local minimum in the TDCS for $\mathbf{k}_s = \boldsymbol{\kappa}$ for which

$$p_{max} = \|\mathbf{q} - \boldsymbol{\kappa}\|. \tag{12}$$

Looking at (8) we see that the cross section is symmetric about the momentum transfer direction, $\mathbf{q}$, and goes like $\frac{1}{q^4}$ as $q \to 0$ in contradiction to the experimentally observed $\frac{1}{q^2}$ [9,20,21]. This spurious behavior arises because we have neglected the effect of the atomic nucleus on the slow electron in the final state but included it in the initial. Indeed in the absence of any interaction the initial and final states are not orthogonal and we have therefore included a non physical auto-ionizing contribution. To correct for this we can assume that the outgoing slow electron is in a continuum state of the ion. We calculate this by treating the slow ejected electron as moving in the static exchange potential of the ion and orthogonalize this state to the bound state. This is the PWDWPW case, with a distortion only on the slow electron. Then the direct scattering amplitude becomes

$$f^{PWDWPW} = (2\pi)^{-9/2} \int d^3r_s d^3r_f \times e^{-i\mathbf{k}_f\cdot\mathbf{r}_f}\chi^-(\mathbf{k}_s,\mathbf{r}_s)\frac{1}{\|\mathbf{r}_f-\mathbf{r}_s\|}e^{i\mathbf{k}_0\cdot\mathbf{r}_f}\psi_{nlm}(\mathbf{r}_s). \tag{13}$$

We can still apply the Bethe relation, (5) to get

$$f^{PWDWPW} = \frac{4\pi}{(2\pi)^{9/2}q^2}\int d^3r_s\chi^-(\mathbf{k}_s,\mathbf{r}_s)e^{i\mathbf{q}\cdot\mathbf{r}_s}\psi_{nlm}(\mathbf{r}_s). \tag{14}$$

If we again neglect exchange amplitude we have the 1st Born approximation:

$$\frac{d^3\sigma^{1stBorn}}{d\Omega_f d\Omega_s dE} = (2\pi)^4\frac{k_f k_s}{k_0}\sum_m |f^{PWDWDW}_{nlm}|^2. \tag{15}$$

We see immediately that the symmetry about the direction of momentum transfer is maintained and also if we expand

$$e^{i\mathbf{q}\cdot\mathbf{r}_s} = 1 + qr_s\cos\mu + O(q^2) \tag{16}$$

where $\mathbf{q}\cdot\mathbf{r}_s = qr_s\cos\mu$, then the orthogonality of $\psi_{nlm}(\mathbf{r}_s)$ and $\chi^-(\mathbf{k}_s,\mathbf{r}_s)$ means that the TDCS has the correct q^{-2} behavior as $q \to 0$. In Zhang et al. [6] it was argued that the distorting effect of the atom, primarily the Coulomb interaction with nucleus could not be neglected for any of the electrons; to represent these effects they calculated the wave function of the slow ejected electron in the static exchange potential of the ion and the incoming and outgoing electrons in the static exchange potential of the atom. We will denote this approximation as DWDWDW, or just DWBA, since this is what is usually meant by the DWBA. We note

- a local exchange approximation of Furness-McCarthy type, [12,20], is used to simplify the static exchange calculation;
- both final state distorted waves are orthogonalized to the ground state;
- no final state electron-electron interaction is included, i.e. the approach is strictly first order in $\frac{1}{\|\mathbf{r}_f-\mathbf{r}_s\|}$. This has been shown to have negligible effect [22];
- the Hartree Fock wave functions of [23] are used for the target wave functions ψ_{nlm}.

In Figure 3 we show a comparison between the older experiments from Hink and his collaborators [6] on Ar($2p$) and the very recent experiments for Mg($3s$), [7], and the DWBA (i.e. DWDWDW). We see for Ar that the theory correctly predicts a binary peak which is split in the forward direction and a recoil peak which is much larger than the binary and also split. For Mg we have a single peak in the direction of momentum transfer. We can understand the splitting of the binary in that the minimum value occurs in the region of $\mathbf{0} = \mathbf{k}_0 - \mathbf{k}_f - \mathbf{k}_s$ exactly as we would expect for a p state. We have a maximum at this point for magnesium since the target electron is in an s state. In order to better understanding the competing process for ionization from a $2p$ state we look at a series of model calculations. By switching on and off the distorting potentials we can look at the effect of elastic scattering on the incident, slow and fast electrons. Returning to (2) we define a series of model calculations for Ar($2p$): $E_f = 500$ eV, $\theta_f = 25°$, $E_s = 200$ eV, Figure 4. These consist of the PWPWPW, the DWBA, PWDWPW, and DWPWPW. The DWPWPW is where we have put a distortion of the fast electron but left the slow and incoming electron as plane waves. Note that in all cases we include exchange and that the distorted waves are orthogonalized to the ground state but the plane waves are not.

The PWPWPW case has a local minima when $\mathbf{k}_s$ is in the $\mathbf{q}$ and $-\mathbf{q}$ directions. These minima arise solely from the $2p$ character of the wave function, as discussed above. The effect of switching on the elastic scattering on the slow ejected electron is to significantly enhance the recoil peak in the PWDWPW case. If however we allow only for elastic scattering of the incoming and fast electrons but not the slow (DWPWDW) the recoil remains small but the binary is reduced. The effect of including elastic scattering on all free particles, (DWBA), is to further enhance the recoil over the binary, as compared to the PWDWPW case. The splitting of the recoil peak is a much clearer structure in the DWBA and should be readily visible in an experiment. The split binary and recoil is seen in all the calculations. We see that distortion is needed in all channels to maximize this effect. It should be remembered that when we included distorted waves in all channels we allow not only for elastic in these channels but also for the distorted waves to interfere [24]. The structures predicted here are similar to those found in the DWBA calculations of [6]. The experimental results of [6,7] are certainly consistent with the DWBA (see Figs. 3, 5). Unfortunately for the choice of kinematics used by [7] it is impossible to distinguish between the simple PWDWPW and the DWBA with a relative measurement.

In Figure 5 we show a comparison between the DWBA and PWDWPW calculations and the experimental data

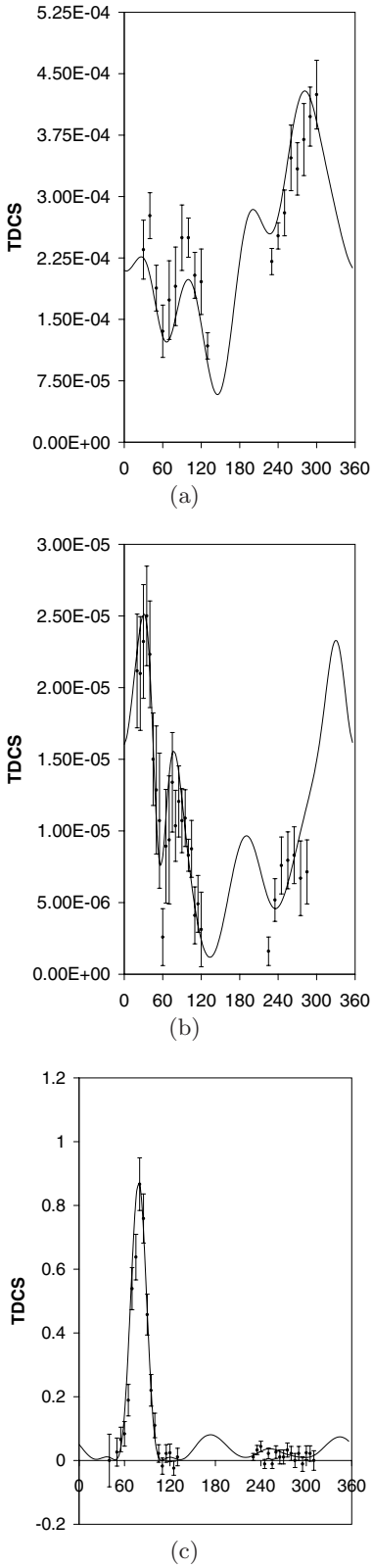

Fig. 3. (a) TDCS for Ar($2p$) $E_0 = 1949$ eV, $E_f = 1550$ eV, $\theta_f = 15.6°$, experiment and theory from [6]. (b) TDCS for AR($2p$) $E_0 = 1949$ eV, $E_f = 1200$ eV, $\theta_f = 30°$, experiment and theory from [6]. (c) TDCS for Mg($3s$), $E_0 = 1027.6$, $E_f = 1000$ eV, $\theta_f = 5°$, experiment from [7]. Solid curve is DWDWDW (i.e. DWBA) for all three cases.

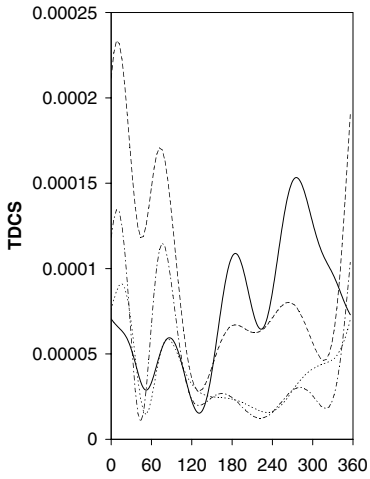

Fig. 4. TDCS (atomic units) for Ar($2p$): $E_f = 500$ eV, $\theta_f = 25°$, $E_s = 200$ eV. Solid curve is DWBA, dotted is DWPWDW (distorted waves in the incident and fast channels), dashed is 1st Born, and dash and dotted is a plane wave 1st Born calculation.

of [7], for Ar($2s$) and Mg($2p$). The experimental data, being relative, has been normalized to the DWBA. Agreement with the DWBA is good, but had we fitted to the PWDWPW agreement would have been equally good. There is a large difference in absolute size between the two approximations in the Ar($2s$) case but the results for the Mg($2p$) are remarkably close both in shape and magnitude. However by making a relatively small change in parameters we can produce cross sections which should be easily distinguishable (see Fig. 6).

It would be extremely useful to have experimental data on an absolute scale. However, as mentioned above, this is probably beyond present experimental capabilities. Hence it is of value to seek out kinematics where the difference between the different theoretical approaches are apparent in the shape of the TDCS, as we have done above. It is also important however to look for a way to systematically inter-normalize different relative measurements. This is particularly true for s states where even in the DWBA the TDCS is relatively structureless. Here the difference between the theories must of course lie in the relative size of the cross section. Several methods for accomplishing this have been suggested [25] in the past. We suggest working in the coplanar constant Θ_{fs} geometry [26]. In this geometry the detectors for the two final state electrons are moved simultaneously so that their mutual angle Θ_{fs} is held constant, see Figure 7, where the TDCS is plotted as a function of θ_s. The effect of performing such an experiment would allow one to place all the coplanar asymmetric measurements done for the same impact and existing energies on the same scale and thus permit a welcome if more severe test of theory.

2 Summary

We have considered the underlying theory for the distorted wave Born approximation and shown that while it

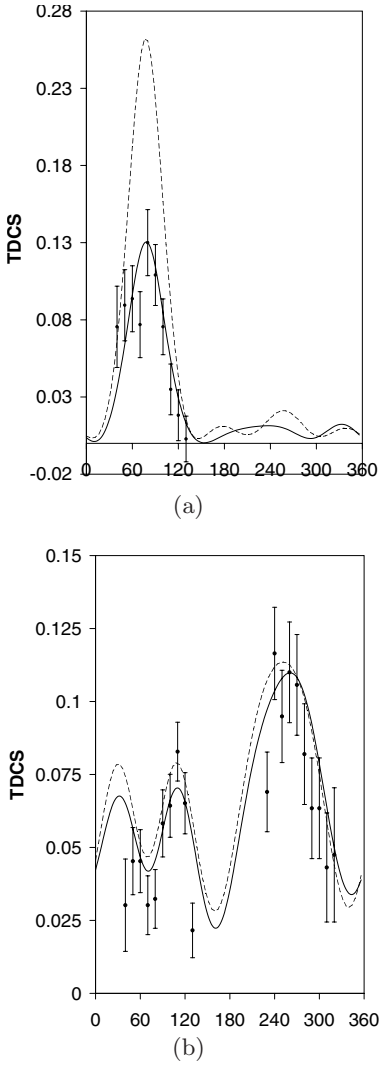

Fig. 5. TDCS (atomic units) for panel (a) Ar($2s$): $E_f = 1000$ eV, $\theta_f = 12^\circ, E_s = 20$ eV; for panel (b) Mg($2p$): $E_0 = 1078$ eV, $E_f = 1000$ eV, $\theta_f = 7^\circ$. Solid line DWBA (i.e. DWDWDW), dotted plane wave 1st Born. Experiment from [7].

generally gives good agreement with the available experimental data, the nature of this data being both relative and over a limited angular range is such that in many cases one is not able to unambiguously distinguish between different theoretical models. We illustrated the idea by considering the very recent experimental results, [7], where the available experimental data is in good agreement with both the 1st Born approximation and the DWBA and showed that by relatively small change in the parameters we could arrive at a situation where a relative experiment should be able to clearly differentiate. We further suggest performing complementary measurements in both coplanar asymmetric and coplanar constant Θ_{fs} geometries, which would allow an inter-normalization between different measurements. We illustrated the idea by considering Ar($2s$). We recommend this measurements to our experimental colleagues.

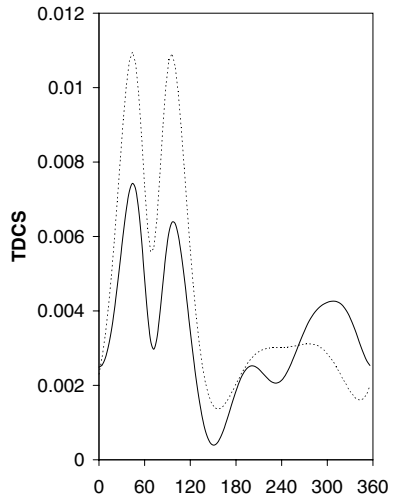

Fig. 6. Coplanar asymmetric geometry for Mg($2p$): $E_0 = 1153$ eV, $E_f = 1000$ eV, $\theta_f = 15^\circ$. Solid curve is DWBA, dotted curve is 1st Born.

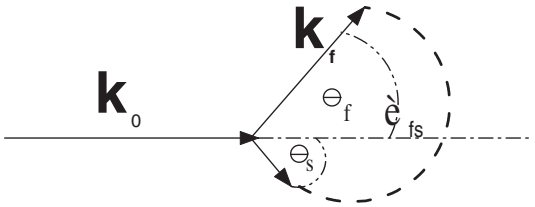

Fig. 7. Coplanar θ_{fs} geometry the mutual angle between the fast and slow scattered electrons is held constant and both are rotated in anti-clockwise direction about the beam direction.

We are most grateful to Dr Lorenzo Avaldi for supplying us with his experimental data prior to journal publication.

Appendix

Here we present a simple derivation of (10) Starting from the general addition theorem for spherical harmonics, [27],

$$P_l(\cos\gamma) = \frac{4\pi}{2l+1}\sum_{m=-l}^{m} Y^*_{lm}(\theta',\phi')Y_{lm}(\theta,\phi) \qquad (17)$$

where

$$\cos\gamma = \cos\theta\cos\theta' + \sin\theta\sin\theta'\cos(\phi-\phi') \qquad (18)$$

consequently if $\theta = \theta', \phi = \phi'$ (17) becomes

$$P_l(1) = \frac{4\pi}{2l+1}\sum_{m=-l}^{m} |Y_{lm}(\theta,\phi)|^2 \qquad (19)$$

but, [28], $P_l(1) = 1 \ \forall\, l$ hence (10) immediately follows.

References

1. This notation means we are looking at the process $e^- + \mathrm{Ar}(1s^2, 2s^2, 2p^6, 3s^2, 3p^6) \rightarrow 2e^- + \mathrm{Ar}(1s^2, 2s^2, 2p^5, 3s^2, 3p^6)$

2. A. Lahmam-Bennani et al., Phys. Rev. A **30**, 1511 (1984)
3. G. Stefani et al., J. Phys. B **19**, 3787 (1986)
4. S. Cavanagh, B. Lohmann, J. Phys. B **30**, L231 (1997)
5. I. Taouil et al., J. Phys. B **32**, L5 (1999)
6. X Zhang et al., J. Phys. B **25**, 4325 (1992) and references cited therein
7. P. Bolognesi et al., in *Proceedings of the 9th European Conference on Atomic and Molecular Physics*, edited by D. Charalambidis, S. Farantos, P. Lambropoulos (E.P.S., 2007), TU1
8. H. Ehrhardt et al., Z. Phys. D **1**, 3 (1986)
9. J. Rasch et al., in *Coincidence Studies of Electron and Photon Impact Ionization*, edited by C.T. Whelan, H.R.J. Walters (Plenum, New York, 1997), p. 305
10. A. Lahmam-Bennani, M. Cherid, A. Duguet, J. Phys. B **20**, 2531 (1987)
11. R.V. Calhoun, D.H. Madison, W.N. Shelton, J. Phys. B **10**, 3523 (1977)
12. J. Rasch, Ph.D. thesis, University of Cambridge, 1996
13. C.T. Whelan et al., in $(e, 2e)$ *and related processes*, edited by C.T. Whelan et al. (Kluwer, Netherlands, 1993)
14. X. Zhang, C.T. Whelan, H.R.J. Walters, J. Phys. B **23**, L509 (1990)
15. S.P. Lucey, J. Rasch, C.T. Whelan, Proc. Roy. Soc. A **455**, 349 (1999)
16. B.H. Bransden, C.J. Joachain, *Physics of Atoms and Molecules* (Prentice Hall, Harlow, 2003)
17. E. Weigold, I.E. McCarthy, *Electron Momentum Spectroscopy* (Kluwer/Plenum, New York, 1999)
18. C.T. Whelan, in $(e, 2e)$ *New Directions in Atomic Physics*, edited by C.T. Whelan et al. (Kluwer/Plenum, New York, 1999), p. 87
19. Hydrogenic momentum space wave functions are known in closed analytic form e.g. [16] $F_{10}(p) = N_{10}(1 + p^2)^{-2}$; $F_{21}(p) = N_{21}(1 + 4p^2)^{-3}$ where the N's are normalization constants; we see at once that $F_{21}(p)$ is exactly 0 at $p = 0$ while $F_{10}(0)$ is maximal
20. J.B. Furness, I.E. McCarthy, J. Phys. **6**, 2280 (1973)
21. H.R.J. Walters, X. Zhang, C.T. Whelan, in $(e, 2e)$ *and Related Processes*, edited by C.T. Whelan et al. (Kluwer Academic, New York, 1993), p. 33
22. C.T. Whelan, R.J. Allan, H.R.J. Walters, J. Phys. IV **3**, 39 (1993)
23. E. Clementi, C. Roetti, At. Data Nucl. Data Tab. **14**, 177 (1974)
24. J. Rasch et al., Phys. Rev. A **56**, 1379 (1997)
25. M. Cherid et al., J. Phys. B **22**, 3483 (1989)
26. C.T. Whelan et al., Phys. Rev. A **50**, 4394 (1994)
27. H.J. Weber, G.B. Arfken, *Essential Mathematical Methods for Physicists* (Elsevier, Amsterdam, 2004)
28. E.T. Copson, *Introduction to the Theory of Functions of a Complex Variable* (Oxford University Press, Oxford, 1935)